Use of waste biomass of common mushroom (*Agaricus bisporus*) as a sorbent for the removal of Reactive Black 5 and Basic Violet 10 dyes from aqueous solutions

Tomasz Jóźwiak*, Urszula Filipkowska, Bartosz Pyko

*Department of Environmental Engineering, University of Warmia and Mazury in Olsztyn, ul. Warszawska 117a,
10-957 Olsztyn, Poland, emails: tomasz.jozwiak@uwm.edu.pl (T. Jóźwiak), urszula.filipkowska@uwm.edu.pl (U. Filipkowska),
bartoszpyko@gmail.com (B. Pyko)*

ABSTRACT

The research investigated the sorption efficiency of two dyes: Reactive Black 5 (RB5) and Basic Violet 10 (BV10), on the waste biomass of common mushroom (*Agaricus bisporus*). The scope of the study included: Fourier-transform infrared spectroscopy analysis of mushroom biomass, study on the effect of pH (pH 2–11) on the sorption efficiency of RB5 and BV10 on mushroom biomass, determination of the sorbent's pH_{PZC} point, study on sorption kinetics (sorption equilibrium time, pseudo-first-order and pseudo-second-order, intramolecular diffusion model) as well as determination of the maximum sorption capacity of the tested sorbents (description of experimental data with Langmuir 1, Langmuir 2, and Freundlich isotherms). Sorption of RB5 and BV10 on mushroom biomass was most effective at pH 2. The sorption equilibrium time for RB5 ranged from 150 to 180 min, and for BV10 it reached 210 min. The data from the sorption kinetics studies were best described by the pseudo-second-order model. The intramolecular diffusion model indicated that the sorption of both RB5 and BV10 on mushroom biomass took place in three main phases, differing in sorption intensity and duration. The sorption capacity of mushroom biomass in relation to the anionic dye RB5 was – q_{max} = 180.6 mg/g and was several times greater than in relation to the cationic dye BV10 – q_{max} = 4.0 mg/g.

Keywords: Sorption; Unconventional sorbents; Common mushroom biomass; Reactive Black 5; Basic Violet 10

1. Introduction

About 10,000 types of dyes are available on the global market, and their total annual production reaches over 800,000 tons (Mg) [1]. Dyes are mainly produced for the needs of the textile, tanning, dyeing, and paper industries. Their considerable quantities are often lost during the process of materials dyeing. Depending on the dyeing technology deployed, from 5% to 50% of the weight of dyes used in the production may end up in the wastewater.

The largest producer of colored wastewater is the textile industry, generating even 200,000 tons (Mg) of colored substances annually that end up in its post-production waters [2], thereby making them particularly hazardous to the environment.

The use of ineffective color wastewater decolorization technologies may result in the release of dyes into the natural environment. In natural water reservoirs, the colored substances limit the inflow of solar radiation to submerged hydrophytes, contributing to their photosynthesis

---

* Corresponding author.

inhibition [3]. In addition, many color substances reduce the efficiency of diffusion of atmospheric oxygen in waters, which, combined with low photosynthesis efficiency, may result in the risk of development of anaerobic conditions in the waters. Additionally, a significant part of dyes as well as products of their partial decomposition (e.g., aromatic amines) may be highly toxic to aquatic organisms [4]. In summary, the use of ineffective methods of wastewater decolorization may ultimately lead to the degradation of the ecosystem of nearby water reservoirs. Therefore, the development and improvement of the color wastewater treatment technology seems to be a priority.

It is commonly believed that sorption is one of the most effective and, at the same time, the most environmentally friendly methods of wastewater decolorization [5–7]. Active carbons are popular and widely used sorbents for wastewater decolorization. Due to the large surface area (500–1,500 m²/g) [8], these materials have good sorption properties in relation to most of the dyes used in the industry. The main disadvantage of active carbons is their high price associated with their high production or regeneration costs. Hence, the search for a cheaper alternative is currently underway in order to make sorption-based technologies economically viable.

Currently, high hopes are fostered with the use of waste materials from the agri-food industry as a raw material for the production of sorbents. Examples of materials that can potentially act as sorbents are the stems and leaves of crops, seed shells, and vegetable and fruit peels [9]. These materials usually exhibit a fairly good binding efficiency of basic dyes. The sorption capacity of waste plant biomass is mainly due to the content of polysaccharides in the biomass (cellulose, hemicellulose, starch) and lignins (tree wood) [10]. The advantage of this type of material is the wide availability and very low price.

Theoretically, waste mushroom biomass can also serve as the sorption material. One of the best known species of cultivated mushrooms is the common mushroom (*Agaricus bisporus*). It is of great economic importance as its global production reaches about 2 million tons (Mg) annually (2019) [11]. In the process of selection and processing of mushroom fruiting bodies, a significant part of the mushroom biomass becomes post-production waste. These are mainly: mushroom tails (lower part of fruiting bodies), broken fragments of fruiting bodies (cap, gills or stem) as well as out-of-class fruiting bodies. These production wastes must be managed.

Mushroom fruiting bodies are made in about 92% of water. Their dry matter is mainly composed of proteins and carbohydrates. The mushroom cell walls contain large amounts of chitin, which accounts for approximately 6%–10% of mushroom dry weight [11,12]. Due to the high content of both proteins and chitin, the waste biomass of mushrooms can potentially be a very good sorbent for both anionic and cationic dyes. In addition, it is widely available in Europe and cheap. Therefore, it can be assumed that this material is an attractive alternative to conventional sorbents.

The study investigated the sorption efficiency of two dyes very popular in the industry: Reactive Black 5 and Basic Violet 10 on waste biomass of mushrooms (*Agaricus bisporus*).

2. Materials

2.1. Common mushroom biomass (Agaricus bisporus)

Waste mushroom biomass from the local cultivation of common mushrooms (*Agaricus bisporus*) (Warmian–Masurian Voivodeship, Poland) was used in the research. The mushroom biomass consisted mainly of: mushroom stems (lower part of the fruiting body), broken pieces of fruiting bodies as well as non-class fruiting bodies. The standard dry matter composition of common mushrooms is as follows: carbohydrates (saccharides) – 53.1%–56.5% (including chitin – 5.9%–8.9%); proteins – 29.1%–36.2%; fats – 1.9%–3.6%; and ash – 9.2%–11.4% [13–15].

2.2. Dyes

Two dyes, very popular in the industry, were used in the research: Reactive Black 5 and Basic Violet 10. The dyes were purchased at the "BORUTA S.A." dye production plant in Zgierz (Łódź Voivodeship, Poland).

Reactive Black 5 (RB5) is an anionic reactive dye. It belongs to the class of diazo dyes and possesses vinylsulfone and sulfone functional groups. Its molecular mass is 991.8 g/mol, whereas its absorption maximum is reached at the wavelength of 600 nm. It is mainly used for dyeing cotton, wool, and polyamide fibers. It can be found under commercial names Remazol Black B, Begazol Black B or Black B. Basic Violet 10 (BV10) is a cationic dye belonging to the class of xanthene dyes. It owes its cationic character to tertiary amine groups. It possesses a carboxyl functional group capable of ionization. Its molecular mass is 479.0 g/mol, and it exhibits absorption maximum at a wavelength of 554 nm. BV10 is used to dye cotton, paper, and leather. Its other commercial names include Rhodamine B or Brilliant Pink B. Structural formulas of both dyes used in the study are depicted in Fig. 1.

2.3. Laboratory equipment

The following laboratory equipment was used during the experiments:

- pH-meter HI 221, Hanna Instruments (USA) – pH measurement and regulation
- UV/VIS spectrophotometer UV-3100PC, VWR (China) – measuring the concentration of dyes in solutions
- multi-station magnetic stirrer MS-53M Magnetic Stirrers, GMI (USA) – sorption of dyes
- laboratory grinder A 11 basic, IKA (China) – grinding mushroom biomass
- FT/IR-4700LE, FTIR Spectrometer with single reflection ATR attachment, JASCO INTERNATIONAL (Japan) – preparation of sorbent Fourier-transform infrared (FTIR) spectra

3. Methodology

3.1. Preparation of sorbent based on waste biomass of common mushroom (CB)

Waste mushroom biomass (fragments of fruiting bodies and caps as well as unclassified fruiting bodies) was cleaned
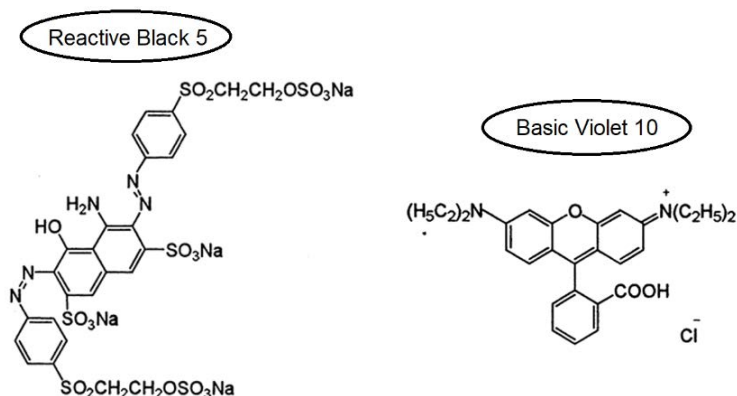
Fig. 1. Structural formulas of Reactive Black 5 and Basic Violet 10 dyes.

of the remains of the subsoil and then washed on a sieve with distilled water. The purified mushroom biomass was crushed in a laboratory grinder and then sieved through laboratory sieves with a mesh size of 2 and 3 mm, respectively. The selected fraction of waste common mushroom biomass with a particle diameter of 2–3 mm (CB) was stored in a sealed container in a laboratory refrigerator (at 4°C).

3.2. Preparation of dye solutions

Stock solutions of dyes (1,000 mg/L) were prepared by dissolving the appropriate amounts of dyes in the powdered form in deionized water. Dye working solutions were prepared by diluting stock solutions with deionized water. The pH of the dye solutions was adjusted by dosing 0.1/1.0 M HCl or 0.1/1.0 M NaOH with continuous pH measurement.

3.3. Research on the influence of pH on the effectiveness of dye sorption

CB (1.0 g_{DM}; assumed dose of sorbent – 2.0 g_{DM}/L) was weighed on a precision balance into a series of beakers (600 mL capacity each). Then, 500 mL of previously prepared working solutions were added to the beakers with dyes at the following concentrations: 10 mg/L (for BV10) or 50 mg/L (for RB5) and subsequent pH values: 2, 3, 4, 5, 6, 7, 8, 9, 10, and 11. The beakers with the solutions were placed on a multi-station magnetic stirrer (200 rpm; the dimensions of the stirrers 8 mm × 40 mm) for 120 min (the assumed mixing parameters guaranteed the mixing of the sorbent in the entire volume of the solution). After the appointed time, samples of the solutions (10 mL) were collected with an automatic pipette into the previously prepared polypropylene test tubes (12 mL volume each). The concentration of dyes in the collected solutions was determined using the spectrophotometric method. The pH of the solutions after sorption was measured as well.

3.4. Studies on the kinetics of dye sorption

CB (2.0 g_{DM}) was weighed to a series of beakers (1,000 mL each) and then dye solutions with the optimal pH (determined based on the results from point 3.3) with

a concentration of 10/50 mg/L (for BV10) or 50/500 mg/L (for RB5) were added to the beakers. The beakers were then placed on multi-station magnetic stirrers (200 rpm). Samples of the solutions (5 mL each) were collected by an automatic pipette at intervals of 0, 10, 20, 30, 45, 60, 90, 120, 150, 180, 210, 240, 270, and 300 min into the previously prepared test tubes (vol. 12 mL). The concentration of dyes was determined spectrophotometrically in all samples at the end of the experiment.

3.5. Research on the maximum dye sorption capacity

Dye solutions with concentrations of: 5, 10, 25, 50, 75, 100, 150, and 200 mg/L (for BV10) or 10, 50, 100, 200, 300, 400, 500, and 600 mg/L (for RB5) and optimal pH (point 3.3) were added to beakers (vol. 600 mL) with weighed CB (1.00 g_{DM} each). Then, the beakers were placed on multi-station magnetic stirrers (200 rpm) for the sorption equilibrium time (determined in point 3.4). After the equilibrium time had elapsed, samples (10 mL) were taken from the beakers for spectrophotometric determination of the concentration of the dye remaining in the solution.

All stages of the research and analyses were carried out at 22°C. The different range of the initial dye concentrations resulted from obvious differences between the sorption efficiency of anionic and cationic dyes on mushroom biomass. However, when planning the research, the series with the concentration of 50 mg/L common for both dyes (point 4.3) was prepared.

3.6. Calculation methods

The amount of dye adsorbed onto CB was determined using Eq. (1):

$$Q_S = (C_0 - C) \times \frac{V}{m} \qquad (1)$$

where Q_S – mass of sorbed dye (mg/g_{DM}); C_0 – initial dye concentration (mg/L); C – the concentration of dye left in the solution after the sorption process (mg/L); V – solution volume (L); m – sorbent mass (g_{DM}).

The kinetics of dye sorption onto CB was described using the pseudo-first-order model (2) [16], the pseudo-second-order

model (3) [16], and the intramolecular diffusion model (simplified intraparticle diffusion model) (4) [17].

$$\frac{\Delta q}{\Delta t} = k_1 \times (q_e - q)$$ (2)

$$\frac{\Delta q}{\Delta t} = k_2 \times (q_e - q)^2$$ (3)

$$q = k_{id} \times t^{0.5}$$ (4)

where q_e – equilibrium amount of sorbed dye (mg/g$_{DM}$); Q – instantaneous mass of adsorbed dye (mg/g$_{DM}$); k_1 – sorption rate constant in the pseudo-first-order model (1/min); k_2 – sorption rate constant in the pseudo-second-order model (g/(mg min)); k_{id} – sorption rate constant in the intramolecular diffusion model (mg/g·min$^{0.5}$); t – sorption time (min).

Experimental data from research upon maximum sorption capacity of waste biomass of mushrooms are described by the Langmuir 1 isotherm (5) [18], Langmuir 2 isotherm (dual-site Langmuir) (6) [19], and Freundlich isotherm (7) [20].

$$q_e = \frac{(q_{max} \times K_C \times C)}{(1 + K_C \times C)}$$ (5)

$$q_e = \frac{(b_1 \times K_1 \times C)}{(1 + K_1 \times C)} + \frac{(b_2 \times K_2 \times C)}{(1 + K_2 \times C)}$$ (6)

$$q_e = K \times C^n$$ (7)

q_e – equilibrium amount of sorbed dye [mg/g DM]; q_{max} – maximal capacity of the monolayer [mg/g DM]; b_1 – maximal capacity of the monolayer (mg/g$_{DM}$); b_1 – maximal capacity of type I active sites in the monolayer (mg/g$_{DM}$); b_2 – maximal capacity of type II active sites in the monolayer (mg/g$_{DM}$); K_1/K_2 – constants in the double Langmuir equation (L/mg); K – constant of the sorption equilibrium in the Freundlich equation; C – the concentration of dye left in the solution after the sorption process (mg/L); n – heterogenicity parameter (Freundlich model).

4. Results and discussion

4.1. FTIR analysis of mushroom waste biomass

The FTIR spectrum of *Agaricus bisporus* waste biomass is typical for mushroom fruiting bodies (Fig. 2). The "stretching vibration" of the O–H bond is responsible for the wide band in the area of 3,500–3,000 cm^{-1}. The peaks at 3,270 and 3,100 cm^{-1} indicate "N–H stretching vibration" of amides A and B of proteins present in the sorbent structure [21]. The peaks at 1,624, 1,546 and 1,260 cm^{-1} indicate the presence of first, second, and third order amides, which also indicates the presence of proteins in the sorbent [22].

The presence of carbonyl groups is confirmed by the peak at 1,420 cm^{-1}, corresponding to the stretching vibration of C=O

[21]. The peaks at 2,850 and 2,920 cm^{-1} represent the symmetric and asymmetric stretching of the CH$_2$ group of fatty acids or unsaturated lipids contained in the sample [22] (Fig. 2).

A series of peaks in the 1,240–900 cm^{-1} range are characteristic of polysaccharides [23]. The saccharide ring stretching vibrations are responsible for the very pronounced peaks at 1,009 and 1,021 cm^{-1}. The peaks at 1,201 and 1,154 cm^{-1} indicate glycosidic C–C and C–O–C bonds, while the peaks at 1,106; 1,059; 951 and 895 cm^{-1} can be attributed to the bending of the C–O–H bond of β-glucans (chitin, mannans, galactans and xylans) [23]. The peak at 1,372 cm^{-1} suggests the presence of an ether bond of the polysaccharides. The peak at 1,309 cm^{-1} is characteristic for the acetamide group of chitin present in the sorbent and is attributed to the stretching of the C–N bond [24,25] (Fig. 2).

4.2. Influence of pH on the sorption effectiveness of dyes on CB

The sorption efficiency of anionic reactive dye RB5 on CB was the highest at pH 2 and decreased with the increase of the initial pH, up to pH 11. The greatest decrease in the efficiency of RB5 binding to CB was noted in the pH range of 3–4 (Fig. 3A).

A similar tendency was observed in the research on RB5 sorption on sawdust [26], cotton fibers [27], chicken feathers [28] or activated carbon [29]. This indicates a similar dye binding mechanism, mainly related to electrostatic interactions between the sorbent surface and the functional groups of the dye.

The high efficiency of RB5 sorption on CB at low pH was due to the anionic nature of the dye. At a very low pH (pH 2), the concentration of hydronium ions (H$_3$O$^+$) in the solution was so high that not only the basic functional groups of proteins and chitin (amino and acetamide), but also the hydroxyl groups of polysaccharides were intensively protonated (–OH + H$_3$O$^+$ → –OH$_2^+$ + H$_2$O). The large total positive charge on the CB surface electrostatically attracted RB5 anions, which significantly intensified dye sorption.

As the pH of the solution increased, the concentration of hydronium ions decreased, which resulted in a decreasing amount of protonated functional groups. At pH > 3, the hydroxyl groups practically did not undergo protonation, while most of the acid functional groups of proteins (carboxyl groups) were deprotonated, which generated negative charges. The significantly reduced total positive charge on the CB surface in the pH 3–4 range explains the significant decrease in the sorption efficiency of RB5 observed in this range.

At pH > 9, most of the amine and acetamide functional groups of CB existed in a non-ionized form, and at pH > 10 hydroxyl groups could be deprotonated (–OH + OH$^-$ → –O$^-$ + H$_2$O). Under these conditions, the CB surface gained a strong total negative charge, which additionally inhibited the binding of RB5 on the sorbent's surface.

The sorption efficiency of BV10 on CB, similar as in case of RB5, was the highest at pH 2 and decreased with increasing pH. However, the influence of pH on the binding efficiency of BV10 was not as significant as it was in the test series with anionic dye (Fig. 3B). A similar effect of pH
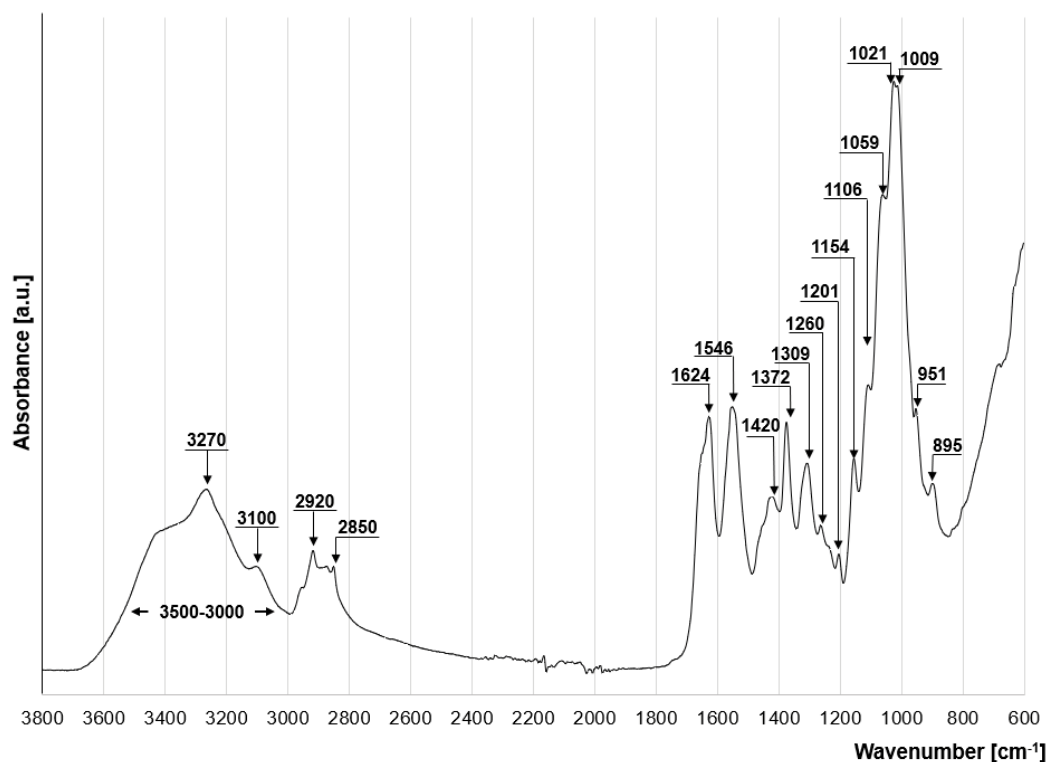
Fig. 2. FTIR spectra of CB.

on dye sorption was noted in the research unto the sorption of BV10 on tea leaves, used coffee beans [30], sawdust [26] and pumpkin seeds [31].

Due to the presence of a carboxylic functional group, Basic Violet 10 is capable of generating a local negative charge in an aqueous solution ($-COOH + H_2O \rightarrow -COO^- + H_3O^+$). Due to this property, despite its generally basic nature, BV10 was able to react similarly to an anionic dye and bind efficiently to the CB surface at low pH.

CB influenced the pH of the dye solution during sorption. In the initial pH range of 4–10, the pH value of the solutions after sorption was established in the range of pH 4.94–6.89 for RB5 and pH 5.05–6.70 for BV10 (Fig. 3C and D). Changes in the pH of solutions during sorption are a phenomenon typical of most sorption processes. The system always strives to obtain a pH at which the sorbent has a total zero charge on its surface (pH_{PZC}). At low pH (below pH_{PZC}), hydrogen cations attach to some functional groups of the sorbent. For example:

$$(-NH_2 + H_3O^+ \rightarrow -NH_3^+ + H_2O)$$

$$(-COO^- + H_3O^+ \rightarrow -COOH + H_2O)$$

$$(-OH + H_3O^+ \rightarrow -OH_2^+ + H_2O)$$
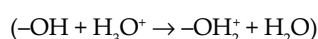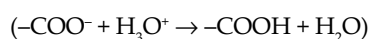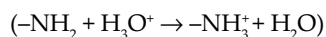
This leads to a decrease in the concentration of hydronium ions in the solution and therefore also to an increase in the pH in the system. On the other hand, at high pH (above pH_{PZC}), protons detach from some of the CB functional groups. For example:

$$(-NH_3^+ + OH^- \rightarrow -NH_2 + H_2O)$$

$$(-COOH + OH^- \rightarrow -COO^- + H_2O)$$

$$(-OH + OH^- \rightarrow -O^- + H_2O)$$
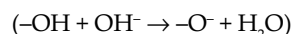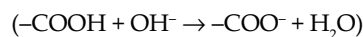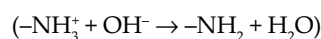
The released hydrogen cations attach to the hydroxyl anions, neutralizing the high pH of the solution.

The pH value of the zero charge point determined for CB with the Boehm titration method was $pH_{PZC} = 5.4$ (Fig. 3E and F). This value suggests that the sorbent is quite acidic.

The next stages of the research were carried out at the optimal sorption pH for each dye (pH 2).

4.3. Sorption kinetics of dyes on CB

The equilibrium time of dye sorption on CB ranged from 150 min (for $C_0 = 50$ mg/L) to 180 min (for $C_0 = 500$ mg/L) in the case of RB5 and reached 210 min (for $C_0 = 10$–50 mg/L) in the case of BV10 (Fig. 4). Sorption of both dyes was the most intense in the first minutes of the process. Already after 30 min the amount of RB5 removed from the system ranged from 76.7% ($C_0 = 500$ mg/L) to 82.8% ($C_0 = 50$ mg/L) of the q_e value, and in case of BV10 – from 51.8% ($C_0 = 50$ mg/L) to 72.9% ($C_0 = 10$ mg/L) of the q_e value (q_e – equilibrium amount of sorbed dye).

The experimental data from the research on the sorption of dyes on CB have been described by pseudo-first-order and pseudo-second-order models (Fig. 4 and Table 1). In each research series, the best fit to the obtained data was shown by the pseudo-second-order model, which is typical for the sorption of organic dyes on biomass-based sorbents [32,33].
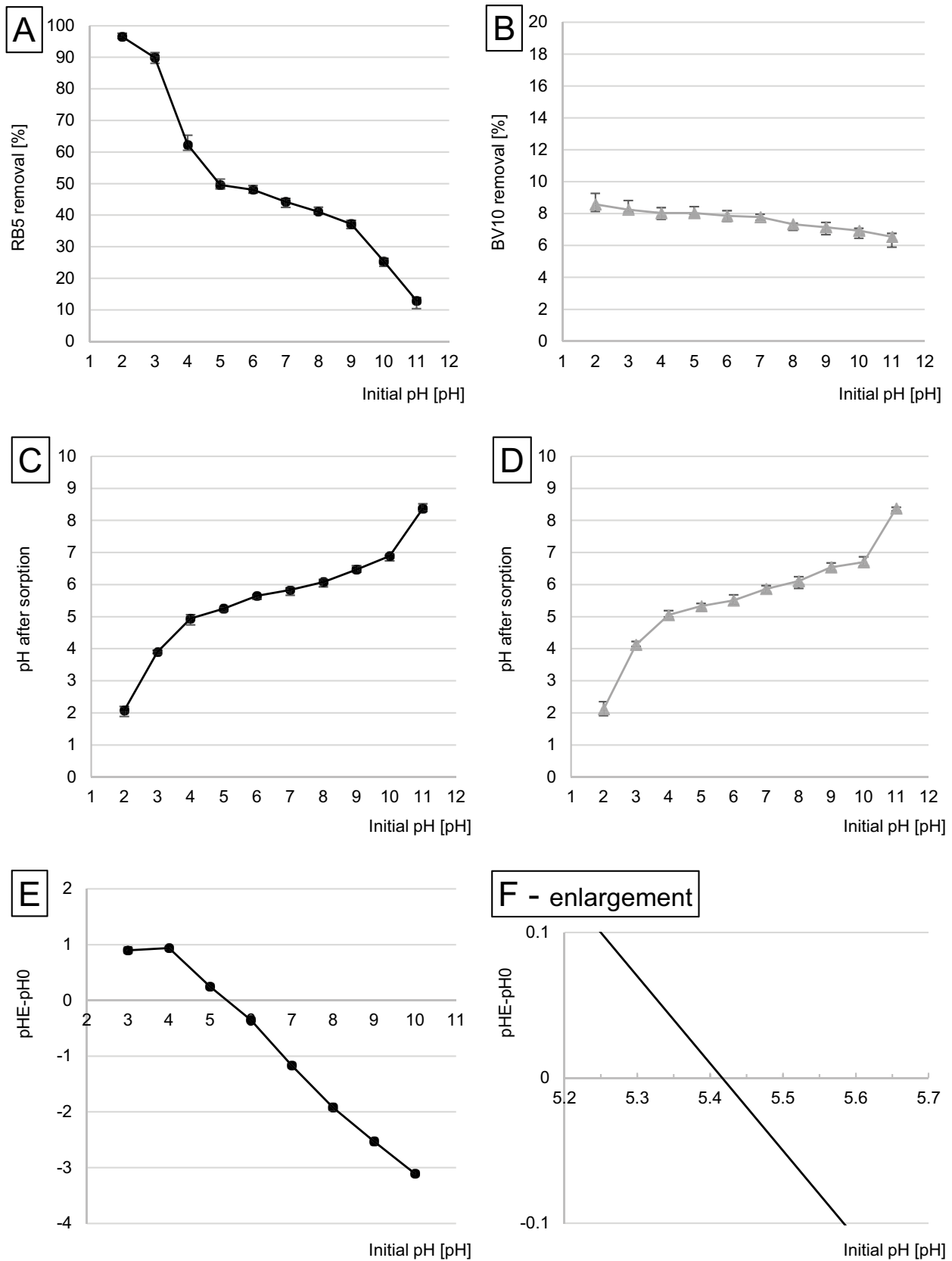
Fig. 3. Effect of pH on the efficiency of sorption of (A) RB5, and (B) BV10 onto CB. Effect of CB on changes in solution pH after sorption of: (C) RB5, and (D) BV10. (E)/(F-enlargement) – Determination of pH_{PZC} of CB with the Boehm's titration method. Temp. 22°C. Experiments were performed in triplicate. Markers denote the mean value and error bars – min. and max. values.
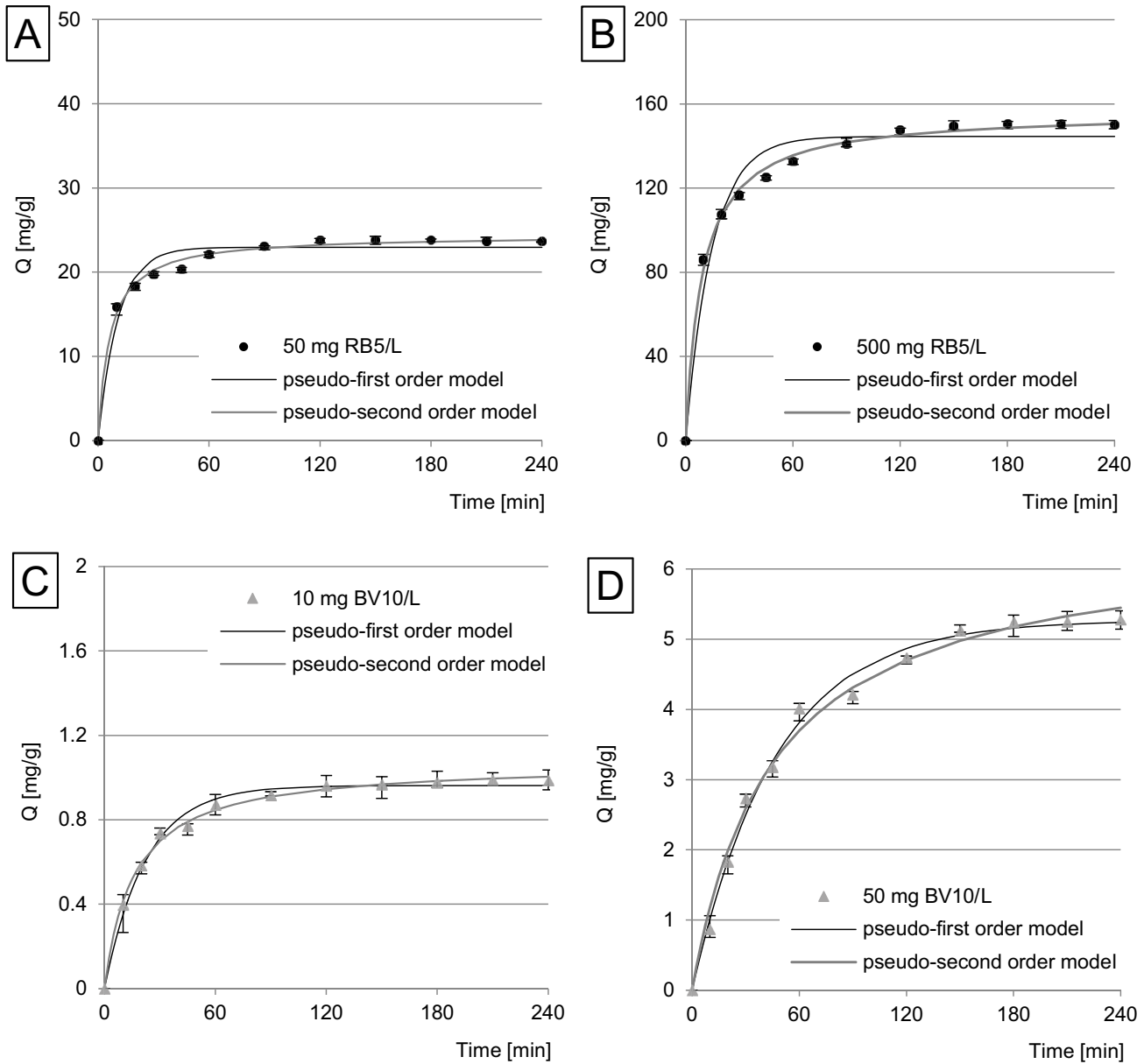
Fig. 4. Kinetics of sorption of: (A) RB5 (50 mg/L), (B) RB5 (500 mg/L), (C) BV10 (10 mg/L), and (D) BV10 (50 mg/L) onto CB. The pseudo-first-order model and the pseudo-second-order model. Temp. 22°C. Experiments were performed in triplicate. Markers denote the mean value and error bars – min. and max. values.

Table 1
Kinetic parameters of RB5 and BV10 sorption onto CB determined from the pseudo-first-order model and pseudo-second-order model

Dye	Dye conc.	Equilibrium time	Exp. data	Pseudo-first-order model			Pseudo-second-order model		
			$q_{e,exp}$	k_1	$q_{e,cal}$	R^2	k_2	$q_{e,cal}$	R^2
	(mg/L)	(min)	(mg/g)	(1/min)	(mg/g)	(–)	(g/(mg·min))	(mg/g)	(–)
RB5	50	150	23.82	0.0924	22.96	0.9663	0.0066	24.43	0.9946
	500	180	149.53	0.0681	144.56	0.9668	0.0007	156.24	0.9965
BV10	10	210	0.98	0.0451	0.96	0.9899	0.0591	1.07	0.9967
	50	210	5.24	0.0214	5.27	0.9914	0.0034	6.47	0.9939

The values of k_2 and q_e determined from the pseudo-second-order model, in the case of both RB5 and BV10 sorption, were very highly dependent on the initial dye concentration. This may indicate a relatively low affinity of both dyes to the CB functional groups (Table 1).

The experimental data was also described with the intramolecular diffusion model. The graphs presented in Fig. 5 show that the sorption process of RB5 and BV10 on CB took place in 3 main phases (Fig. 5 and Table 2).

In the first, the most intense and the shortest phase, the dye molecules probably diffused from the solution onto the sorbent's surface and the sorbate occupied the most accessible active sites. When most of the sorption centers in the CB top layers had been saturated, the second phase began. At this stage, dye molecules competed with each other for the last free sites on the sorbent's surface and began to penetrate into the deeper CB layers. Phase 2 was much less intense than phase 1 and was also longer. In phase 3, the last available active sites in the sorbent's structure were occupied. This sorption phase was characterized by the lowest efficiency due to the small number of free sorption centers and the strong interaction between the dye molecules (Table 2).

The strong relationship between the initial dye concentration and the constants k_{d1}, k_{d2} and k_{d3}, determined from the intramolecular diffusion model, confirms the relatively low
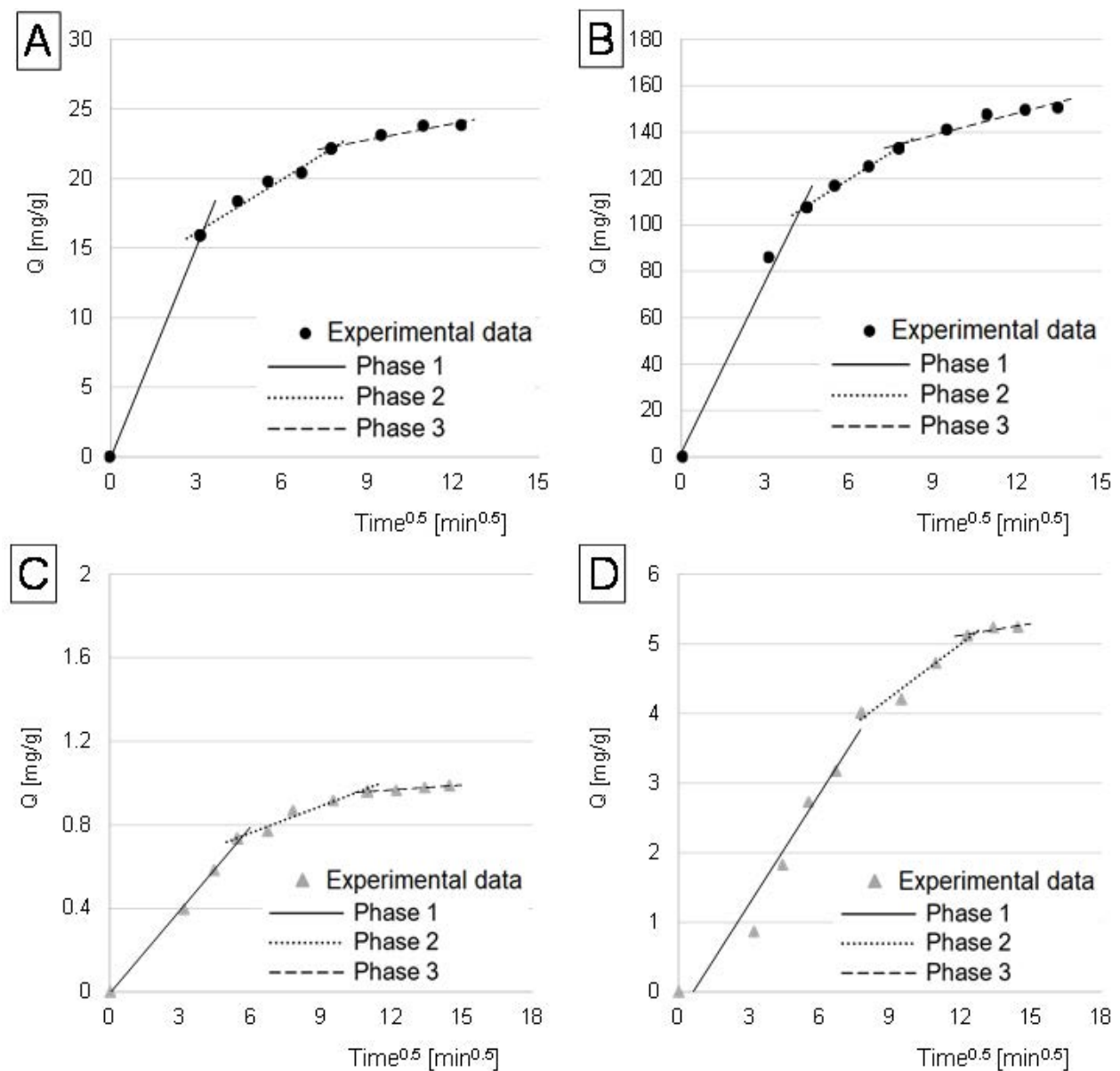

Fig. 5. The intramolecular diffusion model of sorption of: (A) RB5 (50 mg/L), (B) RB5 (500 mg/L), (C) BV10 (10 mg/L), and (D) BV10 (50 mg/L) onto CB. Temp. 22°C. Experiments were performed in triplicate. Markers denote the mean value and error bars – min. and max. values.

affinity of both dyes to CB sorption centers. This suggests that CB's dye sorption capacity will increase along with an increasing dye concentration in the solution.

The much higher efficiency of RB5 sorption on CB compared to BV10 was due to the anionic nature of the Reactive Black 5 dye. At pH 2, RB5 anions were much more electrostatically attracted by the positively charged sorbent surface than the BV10 cations. The stronger electrostatic interaction of RB5 with the CB surface also explains the shorter sorption equilibrium time (Fig. 4 and Table 1) and the shorter duration of the first two key sorption phases on CB (Fig. 5 and Table 2).

4.4. Maximum dye sorption capacity

Experimental data from studies on the maximum dye sorption capacity of CB were described by the Langmuir 1, Langmuir 2 and Freundlich isotherms (Fig. 6 and Table 3).

Table 2
Rate constants of RB5 and BV10 diffusion determined from a simplified intramolecular diffusion model

Dye	Dye conc. (mg/L)	Phase 1			Phase 2			Phase 3		
		k_{d1}	Duration	R^2	k_{d2}	Duration	R^2	k_{d3}	Duration	R^2
RB5	50	5.028	~10	0.9999	1.271	~50	0.9648	0.393	~90	0.9168
	500	24.592	~20	0.9904	7.651	~40	0.9960	3.830	~120	0.9674
BV10	10	0.133	~30	0.9983	0.043	~90	0.9507	0.007	~90	0.9412
	50	0.529	~60	0.9586	0.254	~90	0.9533	0.097	~60	0.9999

Units: k_{d1}, k_{d2}, k_{d3} = (mg/g·min$^{0.5}$); duration (min); R^2 (–).

Table 3
Constants determined from the Langmuir 1 model, Langmuir 2 model and Freundlich model

Dye	Langmuir 1			Langmuir 2						Freundlich		
	q_{max}	K_C	R^2	q_{max}	b_1	K_1	b_2	K_2	R^2	K	n	R^2
	(mg/g)	(L/mg)	(–)	(mg/g)	(mg/g)	(L/mg)	(mg/g)	(L/mg)	(–)	*	(–)	(–)
RB5	159.88	0.078	0.9919	180.59	121.66	0.124	58.93	0.058	0.9967	31.98	0.299	0.9381
BV10	4.00	0.049	0.9858	4.00	2.44	0.049	1.56	0.049	0.9858	0.67	0.338	0.8898

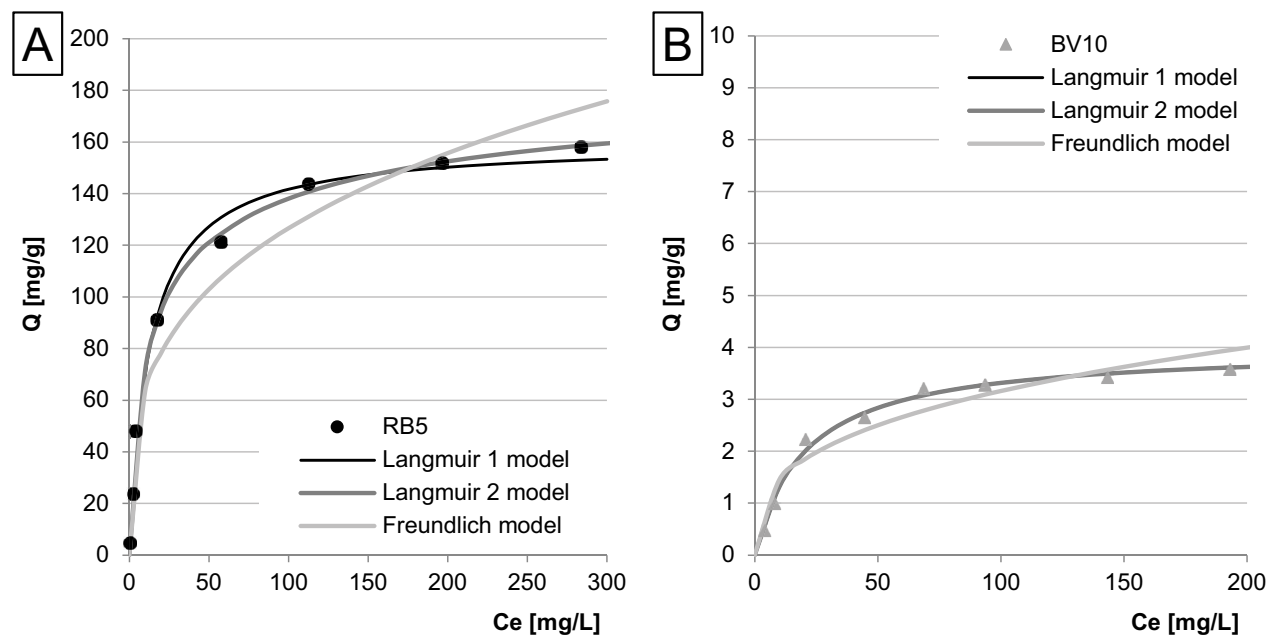*Unit for "K" (Freundlich model) ((mg/g)(L/mg)$^{1/n}$).

Fig. 6. Isotherms of sorption of: (A) RB5 and (B) BV10 onto CB. Temp. 22°C. Experiments were performed in triplicate.

Based on the value of the determination coefficient (R^2), it was found that the sorption of RB5 on CB was best described by the Langmuir double isotherm (Langmuir 2 model) (Table 3). This suggests that at least 2 types of sorption centers play an important role in RB5 sorption. Presumably, the key active sites for the anionic dye RB5 were ionized (protonated) amino functional groups of proteins as well as protonated acetamide and amino chitin groups. Probably, at pH 2, the protonated hydroxyl groups of polysaccharides also played a significant role in RB5 sorption on CB.

Table 4
List of sorption capacities of various sorbents against RB5 and BR46 (literature data)

Dye	Sorbent	q_{max} (mg/g)	Sorption pH	Eq. time (min)	Source
RB5	Chitosan	566.82	4	1,440	[26]
	Chitin	235.65	2	180	[34]
	Common mushroom biomass	180.6	2	180	This work
	Activated carbon in the form of a powder	125.79	2	240	[29]
	Laminaria sp. seaweed biomass	101.5	1	180	[35]
	Tobacco stalk waste biomass	92.84	2	120	[35]
	Activated carbon modified with surfactant	69.9	2	<60	[36]
	Activated carbon (commercial, powder)	58.8	–	–	[37]
	Cotton stems (plant waste)	35.7	1	360	[38]
	Rape stalks	32.8	2.5	120	[39]
	Walnut wood activated carbon	19.3	5	405	[37]
	Wheat straw	15.7	7	195	[40]
	Beech sawdust	13.9	3	1,440	[26]
	Cotton seed shell	12.9	2	30	[41]
	Hen feathers	5.19	2	210	[28]
	Compost	4.8	3	120	[42]
	Fly ash	4.4	5.6	1,440	[43]
	Sunflower seed peel	2.89	3	150	[43]
	Macadamia seed husks	1.21	3	510	[44]
	Sunflower biomass	1.1	2	210	[45]
	Pumpkin seed husks	1	3	60	[31]
	Coconut shells	0.82	2	60	[46]
BV10	Pumpkin seed husks	96	3	60	[31]
	Commercial active carbon powder	72.5	4	1,440	[29]
	Spent coffee grounds	59.3	3	240	[30]
	Active carbon from palm bark	30	3	–	[47]
	Beech sawdust	28.99	3	1,440	[26]
	Coconut shells	28.5	3	180	[46]
	Active carbon from jute fiber	28	8	220	[48]
	Spent green tea leaves	26.7	3	240	[30]
	Baker's yeast	25.2	6.5	72	[49]
	Banana peels	20.6	6	1,440	[50]
	Active fiber from walnut shell	18.7	–	–	[51]
	Coconut fiber	16.5	7	90	[52]
	Sugar cane fiber	10.4	–	–	[53]
	Chitosan	5.9	4	1,440	[29]
	Lemon peel	5.66	3	240	[54]
	Mandarin peel	5.03	3	240	[54]
	Cedar cones	4.6	N.A.	720	[55]
	Common mushroom biomass	4.0	2	210	This work
	Mango leaves (powder)	3.3	N.A.	48	[56]
	Orange peels	3.2	4	–	[50]
	Coffee powder	2.5	2	180	[57]
	Fly ash	1.9	N.A.	72	[43]

In the case of BV10 sorption on CB, the coefficient of determination (R^2) calculated from the Langmuir 1 model had the same value as in the case of Langmuir 2. The same values were also computed for the constants K_1/K_2 and K_C as well as the q_{max} capacity (Table 3). This may suggest the existence of one main sorption center for BV10 or a very similar sorption mechanism common to all types of sorption centers (acetamide, amine and hydroxyl functional groups).

The maximum RB5 sorption capacity of was 180.59 mg/g, and that of BV10 sorption capacity was 4.00 mg/g. The K_1 and K_2 constants determined from the Langmuir 2 model also indicate a greater degree of RB5 affinity to CB compared to BV10.

The high sorption capacity of mushroom biomass in relation to the anionic dye Reactive Black 5 was due to the high content of proteins and chitin in the tested sorbent, which were rich in basic, easily protonated functional groups (amine, acetamide). The much lower sorption capacity of CB relative to BV10 compared to RB5 was probably due to the basic nature of Basic Violet 10. At pH 2, diffusion of BV10 from the solution near the sorbent's surface was hindered by electrostatic repulsion between the protonated CB functional groups and the dye's cations. Presumably, sorption of BV10 on the sorbent's surface occurred only when the deprotonated carboxyl group of the dye approached close enough to the protonated amino, acetamide or hydroxyl group of CB.

Table 4 lists the sorption capacities of various sorbents in relation to the RB5 and BV10 dyes tested in this study.

Mushroom biomass had a greater sorption capacity of the anionic dye RB5 than most unconventional sorbents based on plant biomass (Table 4). Interestingly, the sorption of RB5 onto CB was more efficient than on some types of activated carbons. CB had a similar sorption capacity to the much more expensive pure chitin (Table 4).

CB proved to be an inefficient sorbent of the cationic dye BV10. Much higher BV10 sorption capacity is achieved by sorbents based on waste plant lignocellulosic biomass (Table 4). It should be noted, however, that chitosan, which is one of the best sorption materials for anionic dyes, has a similar BV10 sorption capacity to that of CB.

The study results and the analysis of literature data suggest that mushroom biomass may show better sorption capacity than activated carbons. Theoretically, CB can be successfully used in wastewater treatment from anionic dyes, which are the most common type of contamination of colored industrial wastewater [58].

5. Conclusions

Mushroom biomass can be a very efficient sorbent of the anionic dye RB5 (q_{max} = 180.6 mg/g). However, it proves ineffective in the sorption of the cationic dye BV10 (q_{max} = 4.0 mg/g). The study result is presumably due to the high protein and chitin content in the sorbent. The amino groups present in proteins as well as the amino and acetamide groups present in chitin are the key sorption centers for anionic dyes.

Sorption of dyes on mushroom biomass was based on electrostatic interactions between dye ions and ionized functional groups of the sorbent. For this reason, the pH of the solution played a significant role in the process of dyes binding to CB. In the case of both RB5 and BV10, sorption was most effective at pH 2.

Mushroom biomass caused pH to change during dye sorption. The system always tended to reach the pH value close to the pH$_{PZC}$ of the tested sorbent (pH$_{PZC}$ = 5.4).

Sorption of RB5 and BV10 took place in three main phases, differing in intensity and duration. At pH 2, the equilibrium time of RB5 sorption (150–180 min) on the tested sorbent was shorter than in the case of BV10 (210 min). Presumably, this was due to the strong electrostatic attraction between the positively charged sorbent surface and the RB5 anions.

The better fit of the Langmuir 2 model to the experimental data of RB5 sorption on mushroom biomass compared to the Langmuir 1 model confirms that more than one type of sorption center plays a key role in dye sorption. At pH 2, apart from the aforementioned protonated amino and acetamide groups, also the protonated hydroxyl groups could be important sorption centers.

References

[1] H. Ben Slama, A.C. Bouket, Z. Pourhassan, F.N. Alenezi, A. Silini, H. Cherif-Silini, T. Oszako, L. Luptakova, P. Golińska, L. Belbahri, Diversity of synthetic dyes from textile industries, discharge impacts and treatment methods, Appl. Sci., 11 (2021) 6255, doi: 10.3390/APP11146255.

[2] F.M. Drumond Chequer, G.A.R. de Oliveira, E.R. Anastácio Ferraz, J. Carvalho Cardoso, M.V. Boldrin Zanoni, D.P. de Oliveira, Textile Dyes: Dyeing Process and Environmental Impact, M. Günay, Ed., Eco-Friendly Textile Dyeing and Finishing, InTechOpen, 2013. Available at: https://doi.org/10.5772/53659

[3] B. Lellis, C.Z. Fávaro-Polonio, J.A. Pamphile, J.C. Polonio, Effects of textile dyes on health and the environment and bioremediation potential of living organisms, Biotechnol. Res. Innovation, 3 (2019) 275–290.

[4] C.C. de Jesus Azevedo, R. de Oliveira, P. Suares-Rocha, D. Sousa-Moura, A.T. Li, C.K. Grisolia, G. de Aragão Umbuzeiro, C.C. Montagner, Auramine dyes induce toxic effects to aquatic organisms from different trophic levels: an application of predicted non-effect concentration (PNEC), Environ. Sci. Pollut. Res., 28 (2021) 1866–1877.

[5] D.P. Dutta, R. Venugopalan, S. Chopade, Manipulating carbon nanotubes for efficient removal of both cationic and anionic dyes from wastewater, ChemistrySelect, 2 (2017) 3878–3888.

[6] D.P. Dutta, A. Mathur, J. Ramkumar, A.K. Tyagi, Sorption of dyes and Cu(II) ions from wastewater by sonochemically synthesized MnWO$_4$ and MnMoO$_4$ nanostructures, RSC Adv., 4 (2014) 37027–37035.

[7] A. Singh, D.P. Dutta, J. Ramkumar, K. Bhattacharya, A.K. Tyagi, M.H. Fulekar, Serendipitous discovery of super adsorbent properties of sonochemically synthesized nano BaWO$_4$, RSC Adv., 3 (2013) 22580–22590.

[8] R.S. Jackson, In: R.S. Jackson, Wine Science: Principles and Applications, Elsevier, London, 2020, pp. 573–723.

[9] F. Kallel, F. Chaari, F. Bouaziz, F. Bettaieb, R. Ghorbel, S.E. Chaabouni, Sorption and desorption characteristics for the removal of a toxic dye, methylene blue from aqueous solution

by a low cost agricultural by-product, J. Mol. Liq., 219 (2016) 279–288.

[10] Z. Yan, C. Yi, T. Liu, J. Yang, H. Ma, L. Sha, D. Guo, H. Zhao, X. Zhang, W. Wang, Effect of lignin-containing highly fibrillated cellulose on the adsorption behavior of an organic dye, BioResources, 16 (2021) 6560–6576. Available at: https://webcache.googleusercontent.com/search?q=cache: Hp13NjGhMgMJ:https://ojs.cnr.ncsu.edu/index.php/BioRes/ article/view/BioRes_16_4_6560_Yan_Lignin_Fibrillated_ Cellulose+&cd=2&hl=pl&ct=clnk&gl=pl (Accessed March 31, 2022).

[11] S. Colmenares-Cruz, J.E. Sánchez, J. Valle-Mora, *Agaricus bisporus* production on substrates pasteurized by self-heating, AMB Express, 7 (2017) 135, doi: 10.1186/S13568-017-0438-6.

[12] J. Vetter, Chitin content of cultivated mushrooms *Agaricus bisporus*, *Pleurotus ostreatus* and *Lentinula edodes*, Food Chem., 102 (2007) 6–9.

[13] S. Saiqa, N.B. Haq, A.H. Muhammad, A.A. Muhammad, Ata-ur-Rehman, Studies on chemical composition and nutritive evaluation of wild edible mushrooms, Iran. J. Chem. Chem. Eng., 27 (2008) 151–154.

[14] R. Goyal, R.B. Grewal, R.K. Goyal, Nutritional attributes of *Agaricus bisporus* and *Pleurotus sajor caju* mushrooms, Nutr. Health, 18 (2006) 179–184.

[15] A. Hassainia, H. Satha, S. Boufi, Chitin from *Agaricus bisporus*: extraction and characterization, Int. J. Biol. Macromol., 117 (2018) 1334–1342.

[16] E.D. Revellame, D.L. Fortela, W. Sharp, R. Hernandez, M.E. Zappi, Adsorption kinetic modeling using pseudo-first-order and pseudo-second-order rate laws: a review, Cleaner Eng. Technol., 1 (2020) 100032, doi: 10.1016/J.CLET.2020.100032.

[17] F.C. Wu, R.L. Tseng, R.S. Juang, Initial behavior of intraparticle diffusion model used in the description of adsorption kinetics, Chem. Eng. J., 153 (2009) 1–8.

[18] M.A. Islam, M.A. Chowdhury, M.S.I. Mozumder, M.T. Uddin, Langmuir adsorption kinetics in liquid media: interface reaction model, ACS Omega, 6 (2021) 14481–14492.

[19] G. Yue, H. Wu, J. Yue, M. Li, C. Zeng, W. Liang, Adsorption measurement and dual-site Langmuir model II: modeling and prediction of carbon dioxide storage in coal seam, Energy Explor. Exploit., 37 (2019) 1268–1285.

[20] N. Ayawei, A.N. Ebelegi, D. Wankasi, Modelling and interpretation of adsorption isotherms, J. Chem., 2017 (2017) 3039817, doi: 10.1155/2017/3039817.

[21] G. Bekiaris, D. Tagkouli, G. Koutrotsios, N. Kalogeropoulos, G.I. Zervakis, Pleurotus mushrooms content in glucans and ergosterol assessed by ATR-FTIR spectroscopy and multivariate analysis, Foods, 9 (2020) 535, doi: 10.3390/FOODS9040535.

[22] W. Kukula-Koch, M. Grzybek, A. Strachecka, A. Jaworska, A. Ludwiczuk, ATR-FTIR-based fingerprinting of some Cucurbitaceae extracts: a preliminary study, Acta Soc. Bot. Pol., 87 (2018), doi: 10.5586/asbp.3579.

[23] A.A. Sulieman, K.X. Zhu, W. Peng, H.A. Hassan, M. Obadi, M.I. Ahmed, H.M. Zhou, Effect of *Agaricus bisporus* polysaccharide flour and inulin on the antioxidant and structural properties of gluten-free breads, J. Food Meas. Charact., 13 (2019) 1884–1897.

[24] D. Kumar, J. Pandey, P. Kumar, Synthesis and characterization of modified chitosan via microwave route for novel antibacterial application, Int. J. Biol. Macromol., 107 (2018) 1388–1394.

[25] E.M. Dahmane, M. Taourirte, N. Eladlani, M. Rhazi, Extraction and characterization of chitin and chitosan from *Parapenaeus longirostris* from Moroccan Local Sources, Int. J. Polym. Anal. Charact., 19 (2014) 342–351.

[26] P. Szymczyk, U. Filipkowska, T. Jóźwiak, M. Kuczajowska-Zadrożna, Use of sawdust immobilised on chitosan for disposal of dyes from water solutions, Prog. Chem. Appl. Chitin Deriv., 22 (2017) 207–219, doi: 10.15259/PCACD.22.21.

[27] T. Jóźwiak, U. Filipkowska, S. Brym, M. Zyśk, The use of aminated cotton fibers as an unconventional sorbent to remove anionic dyes from aqueous solutions, Cellulose, 27 (2020) 3957–3969.

[28] T. Jóźwiak, U. Filipkowska, P. Marciniak, Use of hen feathers to remove Reactive Black 5 and Basic red 46 from aqueous solutions, Desal. Water Treat., 232 (2021) 129–139.

[29] U. Filipkowska, T. Jóźwiak, P. Szymczyk, M. Kuczajowska-Zadrożna, The use of active carbon immobilised on chitosan beads for RB5 and BV10 dye removal from aqueous solutions, Prog. Chem. Appl. Chitin Deriv., 22 (2017) 14–26, doi: 10.15259/ PCACD.22.02.

[30] T. Jóźwiak, U. Filipkowska, J. Struk-Sokołowska, K. Bryszewski, K. Trzciński, J. Kuźma, M. Ślimkowska, The use of spent coffee grounds and spent green tea leaves for the removal of cationic dyes from aqueous solutions, Sci. Rep. 111, 11 (2021) 1–12.

[31] A. Kowalkowska, T. Jóźwiak, Utilization of pumpkin (*Cucurbita pepo*) seed husks as a low-cost sorbent for removing anionic and cationic dyes from aqueous solutions, Desal. Water Treat., 171 (2019) 397–407.

[32] M. Hubbe, S. Azizian, S. Douven, Implications of apparent pseudo-second-order adsorption kinetics onto cellulosic materials: a review, BioResorces, 14 (2019) 7582–7626.

[33] Z. Chen, H. Deng, C. Chen, Y. Yang, H. Xu, Biosorption of malachite green from aqueous solutions by *Pleurotus ostreatus* using Taguchi method, J. Environ. Health Sci. Eng., 12 (2014) 63, doi: 10.1186/2052-336X-12-63.

[34] U. Filipkowska, T. Jóźwiak, P. Bugajska, M. Kuczajowska-Zadrożna, The influence of chitin amination on the effectiveness of RB5 and RY84 dye sorption, Prog. Chem. Appl. Chitin Deriv., 23 (2018) 66–75.

[35] K. Vijayaraghavan, Y.S. Yun, Biosorption of C.I. Reactive Black 5 from aqueous solution using acid-treated biomass of brown seaweed *Laminaria* sp., Dyes Pigm., 3 (2008) 726–732.

[36] G.M. Nabil, N.M. El-Mallah, M.E. Mahmoud, Enhanced decolorization of Reactive Black 5 dye by active carbon sorbent-immobilized-cationic surfactant (AC-CS), J. Ind. Eng. Chem., 20 (2014) 994–1002.

[37] Z. Eren, F.N. Acar, Adsorption of Reactive Black 5 from an aqueous solution: equilibrium and kinetic studies, Desalination, 194 (2006) 1–10.

[38] Ö. Tunç, H. Tanaci, Z. Aksu, Potential use of cotton plant wastes for the removal of Remazol black B reactive dye, J. Hazard. Mater., 163 (2009) 187–198.

[39] Y. Hamzeh, A. Ashori, E. Azadeh, A. Abdulkhani, Removal of Acid orange 7 and Remazol black 5 reactive dyes from aqueous solutions using a novel biosorbent, Mater. Sci. Eng., C, 32 (2012) 1394–1400.

[40] W. Zhang, H. Yan, H. Li, Z. Jiang, L. Dong, X. Kan, H. Yang, A. Li, R. Cheng, Removal of dyes from aqueous solutions by straw based adsorbents: batch and column studies, Chem. Eng. J., 168 (2011) 1120–1127.

[41] D. Uçar, B. Armağan, The removal of Reactive Black 5 from aqueous solutions by cotton seed shell, Water Environ. Res., 84 (2012) 323–327.

[42] T. Jóźwiak, U. Filipkowska, J. Rodziewicz, A. Mielcarek, D. Owczarkowska, Application of compost as a cheap sorbent for dyes removal from aqueous solutions | Zastosowanie kompostu jako taniego sorbentu do usuwania barwnik?w z roztwor?w wodnych, Rocz. Ochr. Sr., 15 (2013).

[43] P. Pengthamkeerati, T. Satapanajaru, N. Chatsatapattayakul, P. Chairattanamanokorn, N. Sananwai, Alkaline treatment of biomass fly ash for reactive dye removal from aqueous solution, Desalination, 261 (2010) 34–40.

[44] M.M. Felista, W.C. Wanyonyi, G. Ongera, Adsorption of anionic dye (Reactive Black 5) using macadamia seed husks: kinetics and equilibrium studies, Sci. Afr., 7 (2020) e00283, doi: 10.1016/J. SCIAF.2020.E00283.

[45] J.F. Osma, V. Saravia, J.L. Toca-Herrera, S.R. Couto, Sunflower seed shells: a novel and effective low-cost adsorbent for the removal of the diazo dye Reactive Black 5 from aqueous solutions, J. Hazard. Mater., 147 (2007) 900–905.

[46] T. Jóźwiak, U. Filipkowska, P. Bugajska, T. Kalkowski, The use of coconut shells for the removal of dyes from aqueous solutions, J. Ecol. Eng., 19 (2018) 129–135.

[47] M. Mohammadi, A.J. Hassani, A.R. Mohamed, G.D. Najafpour, Removal of rhodamine b from aqueous solution using palm shell-based activated carbon: adsorption and kinetic studies, J. Chem. Eng. Data, 55 (2010) 5777–5785.

[48] K. Porkodi, K. Vasanth Kumar, Equilibrium, kinetics and mechanism modeling and simulation of basic and acid dyes sorption onto jute fiber carbon: Eosin yellow, malachite green and crystal violet single component systems, J. Hazard. Mater., 143 (2007) 311–327.

[49] M.S. Mahmoud, Decolorization of certain reactive dye from aqueous solution using Baker's Yeast (*Saccharomyces cerevisiae*) strain, HBRC J., 12 (2016) 88–98.

[50] C. Namasivayam, N. Kanchana, R.T. Yamuna, Waste banana pith as adsorbent for the removal of rhodamine-B from aqueous solutions, Waste Manage., 13 (1993) 89–95.

[51] S. Kaur, T.P.S. Walia, I. Kansal, Removal of Rhodamine-B by adsorption on walnut shell charcoal, J. Surf. Sci. Technol., 24 (2008) 179–193.

[52] M.V. Sureshkumar, C. Namasivayam, Adsorption behavior of Direct Red 12B and Rhodamine B from water onto surfactant-modified coconut coir pith, Colloids Surf., A, 317 (2008) 277–283.

[53] H. Parab, M. Sudersanan, N. Shenoy, T. Pathare, B. Vaze, Use of agro-industrial wastes for removal of basic dyes from aqueous solutions, Clean – Soil, Air, Water, 37 (2009) 963–969.

[54] T. Józwiak, U. Filipkowska, P. Zajko, Use of citrus fruit peels (grapefruit, mandarin, orange, and lemon) as sorbents for the removal of Basic Violet 10 and Basic red 46 from aqueous solutions, Desal. Water Treat., 163 (2019) 385–397.

[55] M. Zamouche, O. Hamdaoui, Sorption of Rhodamine B by cedar cone: effect of pH and ionic strength, Energy Procedia, 18 (2012) 1228–1239.

[56] T.A. Khan, S. Sharma, I. Ali, Adsorption of Rhodamine B dye from aqueous solution onto acid activated mango (*Magnifera indica*) leaf powder: equilibrium, kinetic and thermodynamic studies, J. Toxicol. Environ. Health Sci., 3 (2011) 286–297.

[57] K. Shen, M.A. Gondal, Removal of hazardous Rhodamine dye from water by adsorption onto exhausted coffee ground, J. Saudi Chem. Soc., 21 (2017) S120–S127.

[58] S. Papić, N. Koprivanac, A. Lončarić Božić, A. Meteš, Removal of some reactive dyes from synthetic wastewater by combined Al(III) coagulation/carbon adsorption process, Dyes Pigm., 62 (2004) 291–298.